Izvestiya, Physics of the Solid Earth, Vol. 36, No. 7, 2000, pp. 553–564. Translated from Fizika Zemli, No. 7, 2000, pp. 31–42.

Geomagnetic Field Variations before and after the Matuyama–Jaramillo Reversal in Western Turkmenistan

G. Z. Gurarii*, V. I. Bagin, A. V. Garbuzenko*, M. Yu. Reshetnyak**, V. M. Trubikhin*, and Kh. Nazarov†*****

** Geological Institute, Russian Academy of Sciences, Pyzhevskii per. 7, Moscow, 109017 Russia; e-mail: palmag@glas.apc.org*
*** Schmidt United Institute of Physics of the Earth, Russian Academy of Sciences, Bol'shaya Gruzinskaya ul. 10, Moscow, 123810 Russia*
**** Institute of Geology, Academy of Sciences of Turkmenistan, ul. Gogolya 16, Ashkhabad, 744600 Turkmenistan*

Received September 20, 1999

Abstract—Based on the maximum entropy and integral wavelet methods, processing of the stationary geomagnetic field of the Matuyama chron prior to the Matuyama–Jaramillo reversal and of the Jaramillo subchron provided the field variation spectrum similar to that derived from archaeomagnetic investigations. However, the time stability analysis of these spectra using their wavelet diagrams rejected some of the inferred periodicities which may reflect singular features and quasi-periodic behavior of the series under study. The spectra that were reliably inferred are discrete and often dissimilar for different field components and time intervals, which may be evidence of a change in the geodynamo operation mode during the reversal.

INTRODUCTION

This paper presents the results on secular variations in the stable-polarity geomagnetic field of the Matuyama chron and Jaramillo subchron near the Matuyama–Jaramillo reversal, obtained within the framework of our combined study of stable-polarity and reversal fields. This work, actually continuing the paper by Gurarii *et al.* [2000], addresses variations in the declination, inclination, and intensity of the geomagnetic field within a wide range of periods (from a few hundred to a few thousand years) and compares the inferred characteristics with variations in the scalar magnetic parameters of rocks studied.

An important feature of the processes considered below (be it the geomagnetic field behavior or factors responsible for the variations in rock characteristics) is the possible nonstationarity of their time spectra. Therefore, the direct application of traditional spectral methods is, generally speaking, invalid in this case. Presently, there are no reasons to believe that spectra of geomagnetic (climatic, and so on) processes with characteristic times of about 10^5 years are due to factors that are "stationary" in time. In such a situation, the interval under consideration is usually divided into a few shorter intervals, and Fourier (or maximum entropy) spectra are constructed for each of the latter. If the resulting spectral peaks are insensitive to the subdivision, the spectrum is considered stationary. A drawback of such an approach is the fact that results of the analysis depend on the mode of the interval subdivision; moreover, the response of each peak to the subdivision is unique. This problem also remains unsolved within the framework of the spectral variation analysis [Nikolaev and Gamburtsev, 1994], using a moving window in the Fourier analysis. In this case, the main difficulty is the decomposition of a nonstationary process over a "stationary" basis. To study processes whose spectra are nonstationary in time, geophysicist Morle and mathematician Gilbert developed, in the mid-1980s, the wavelet analysis, which provides an effective means for studying the time evolution of spectra [Holschneider, 1995; Torresani, 1995; and others]. Note that this method is applicable to time series with data gaps [Galyagin and Frik, 1996] (see also its application to paleomagnetic [Galyagin *et al.*, 1998] and archaeomagnetic [Burakov *et al.*, 1998] data).

ROCKS STUDIED

We analyzed time series of declination (D), inclination (I), and relative intensity of the field; initial magnetic susceptibility of rocks (κ); and normal remanence arising in samples after the application of a constant magnetic field with an intensity of 0.8 T ($IRM_{0.8}$). Geologic, mineralogical, and magnetic mineralogy characteristics of the rocks studied, their time correlation, methods of data acquisition, and data themselves were

† Deceased.

described in detail by Gurarii *et al.* [2000]. Here, we think it necessary to make the following comments.

1. The aforementioned time series were obtained from the study of the two following collections: samples taken from the Matuyama chron zone preceding the Matuyama–Jaramillo reversal and from the Jaramillo subchron zone (profiles 1M and 1J); and samples from a detailed sampling interval in each of the above chron zones (profiles 2M and 2J, respectively).

2. The average sampling interval in profile 1 was 0.5 m (65 and 74 samples from the Matuyama and Jaramillo chron zones, respectively). Profile 2 was sampled nearly continuously with an interval of 2.5 cm, allowing for the losses during cutting handle samples into 2.0-cm cubes. Samples were taken from 255 levels on profile 2M and from 237 levels on profile 2J.

3. The improved correlation of the study section with the magnetochronological scale [Berggren *et al.*, 1995] suggests that the samples of profile 1M are taken with a 174-kyr interval, and those of profile 1F, with a 1.0-kyr interval; the equivalent time intervals of sampling profile 2 in the Matuyama and Jaramillo chron zones are 47 and 38 years, respectively. Therefore, the data from profile-1 samples allow the study of variations as long as 10 to 100 kyr, and the data from profile-2, a few hundred to a few thousand years.

4. The geomagnetic field direction characteristics were taken to be directions of the characteristic component of the natural remanent magnetization (NRM), averaged over five samples for each level; the characteristic component was derived from the component analysis of data obtained from the stepped thermal demagnetization of samples. The NRM characteristic component direction could be compared with that of the field existing in the study area during the accumulation of rocks because their magnetization has a detrital origin [Gurarii *et al.*, 2000]. The inferred directions are characterized, with rare exceptions, by the high accuracy of their determination: the average intrabed precision parameters are $k = 162.0$ with $\alpha_{95} \le 5°$.

5. Relative variations in the field intensity were characterized in terms of the ratio $(NRM_{300°}–NRM_{500°})/(IRM_{300°}–IRM_{500°})$ denoted below as $Rns = \Delta NRM/\Delta IRM$. The NRM values were averaged over five samples, and the laboratory magnetization was determined for one sample of each sampling level.

The series that were analyzed are shown in Figs. 1 and 2.

METHOD OF ANALYSIS

The inferred data series were analyzed using the maximum entropy method (MEM) [Burg, 1968] and wavelet analysis [Holschneider, 1995]. At the first stage of the MEM application, five to ten different filter lengths m, ranging from 30% to 70% of the total series length, were used in order to identify main periods of harmonic oscillations, the sum of which approximates the series studied. The method of quickest descent was then employed to refine the period values and to determine amplitudes, their 90% significance levels, and phase characteristics of the inferred oscillations [Filippov, 1985]. The same data series were treated in terms of the wavelet analysis, whose basic principles are briefly stated below.

Wavelets represent the family of oscillating self-similar functions of various scales localized in both physical and Fourier spaces [Holschneider, 1995; Torresani, 1995]. The wavelet analysis is applicable to the study of spectrally nonstationary processes, the determination of phase variations in components of a quasi-stationary process, and the estimation of its amplitude characteristics. The resulting spectra, in which multiple and combination frequencies are suppressed, are smoother than Fourier spectra.

The continuous wavelet transform of a function is defined as

$$w(a, t) = a^{-1} \int_{-\infty}^{\infty} \psi\left(\frac{t' - t}{a}\right) f(t')dt', \qquad (1)$$

where a is a parameter characterizing the oscillation period; t is time; and $\psi(t)$ is a function, called the analyzing wavelet, that obeys the condition

$$C_\psi = \int_{-\infty}^{\infty} |\omega|^{-1} |\tilde{\psi}(\omega)|^2 d\omega, \qquad (2)$$

ensuring the uniqueness and invertibility of the transformation, where $\tilde{\psi}(\omega) = \int_{-\infty}^{\infty} \psi(t) e^{-i\omega t} dt$ is the Fourier image of the Fourier image of the function $\psi(t)$. Condition (2) leads to the constraint $\int_{-\infty}^{\infty} \psi(t)dt = 0$; i.e., the wavelet average is zero.

The wavelet transformation maps a function of one variable into the plane of two variables t and a. The corresponding analogue of the Fourier spectrum is the so-called integral wavelet spectrum obtained by integrating the squared modulus of the wavelet transform over the time interval under consideration T: $S(a) = T^{-1} \int_0^T |w(a, t)|^2 dt$. The wavelet form is chosen with regard to a specific problem solved in terms of the wavelet analysis. Below, we use the Morle wavelet $\psi(t) = e^{-t^2/2} e^{i2\pi t}$, commonly applied to problems of the spectral analysis.

RESULTS OF THE SPECTRAL ANALYSIS

A. *Results of the MEM analysis*. Most of the inferred MEM peaks are nearly insensitive to the filter

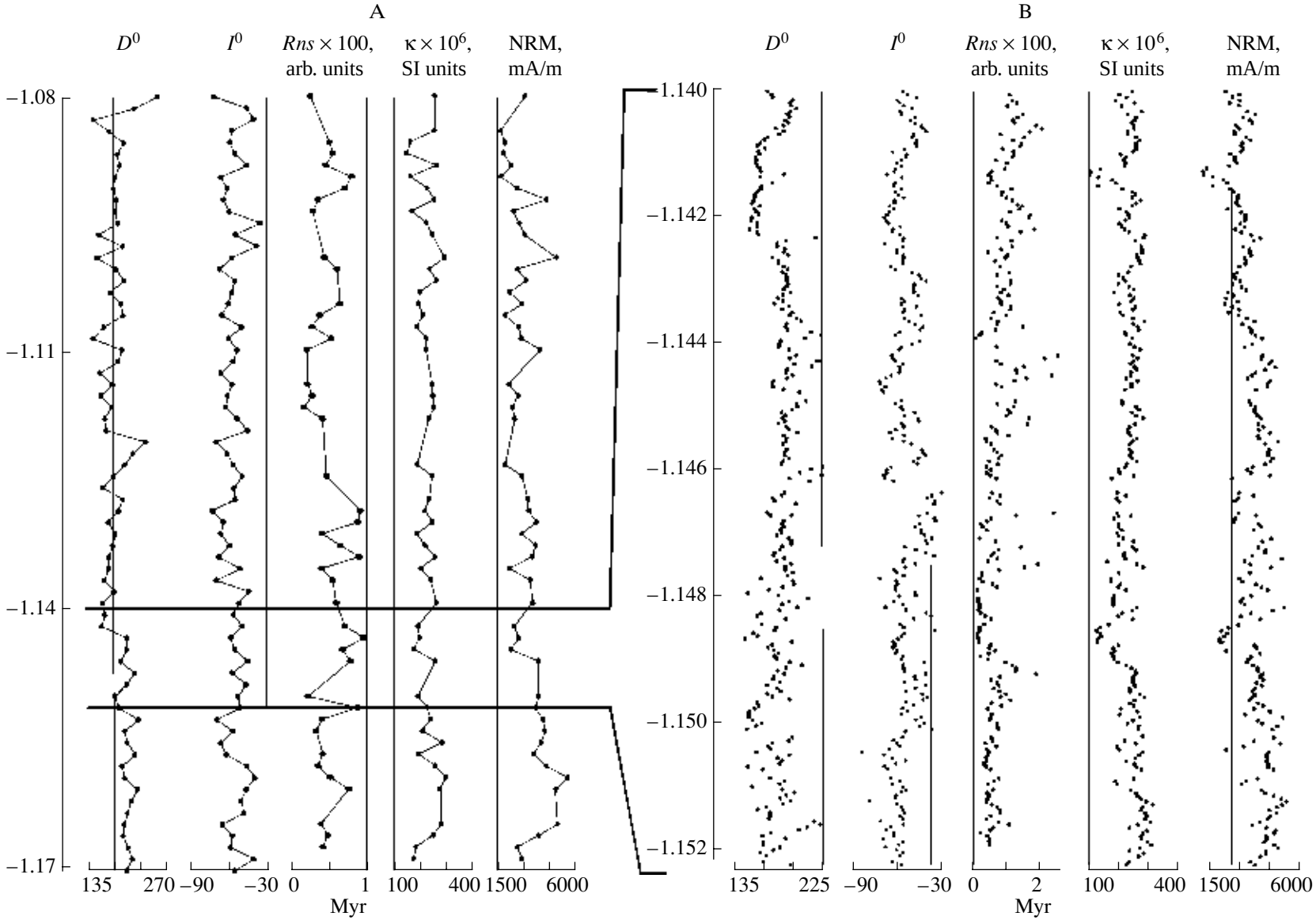

Fig. 1. Paleomagnetic and magnetic characteristics of the Matuyama rocks: A, profile 1; B, profile 2. *D* and *I* are the declination and inclination, *Rns* = ΔNRM/ΔIRM; κ is the magnetic susceptibility, and IRM is the normal magnetization in a 0.8-T field. The position of the profile-2 section is shown relative to profile 1.

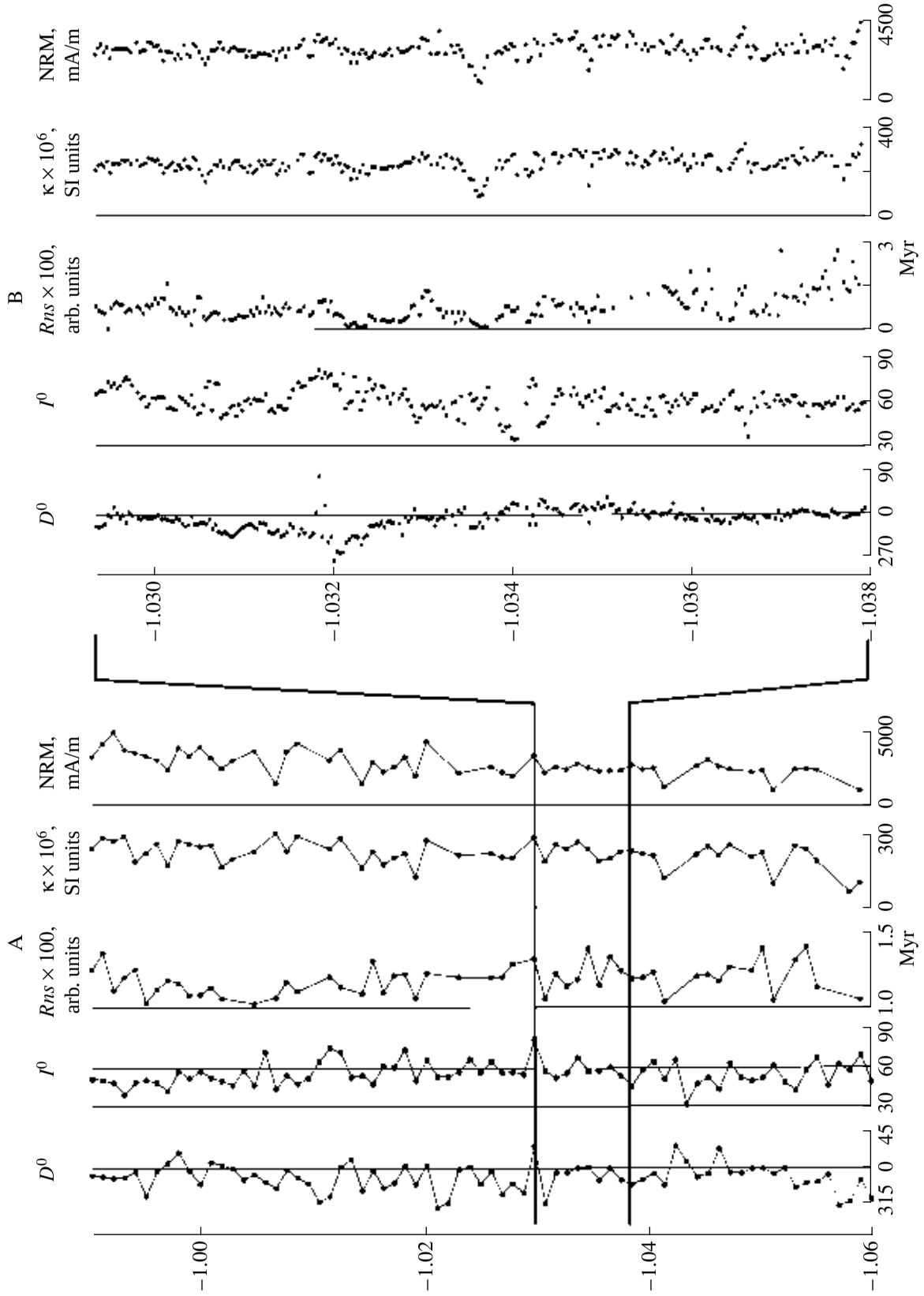

Fig. 2. Paleomagnetic and magnetic characteristics of the Jaramillo rocks. The notation is the same as in Fig. 1.

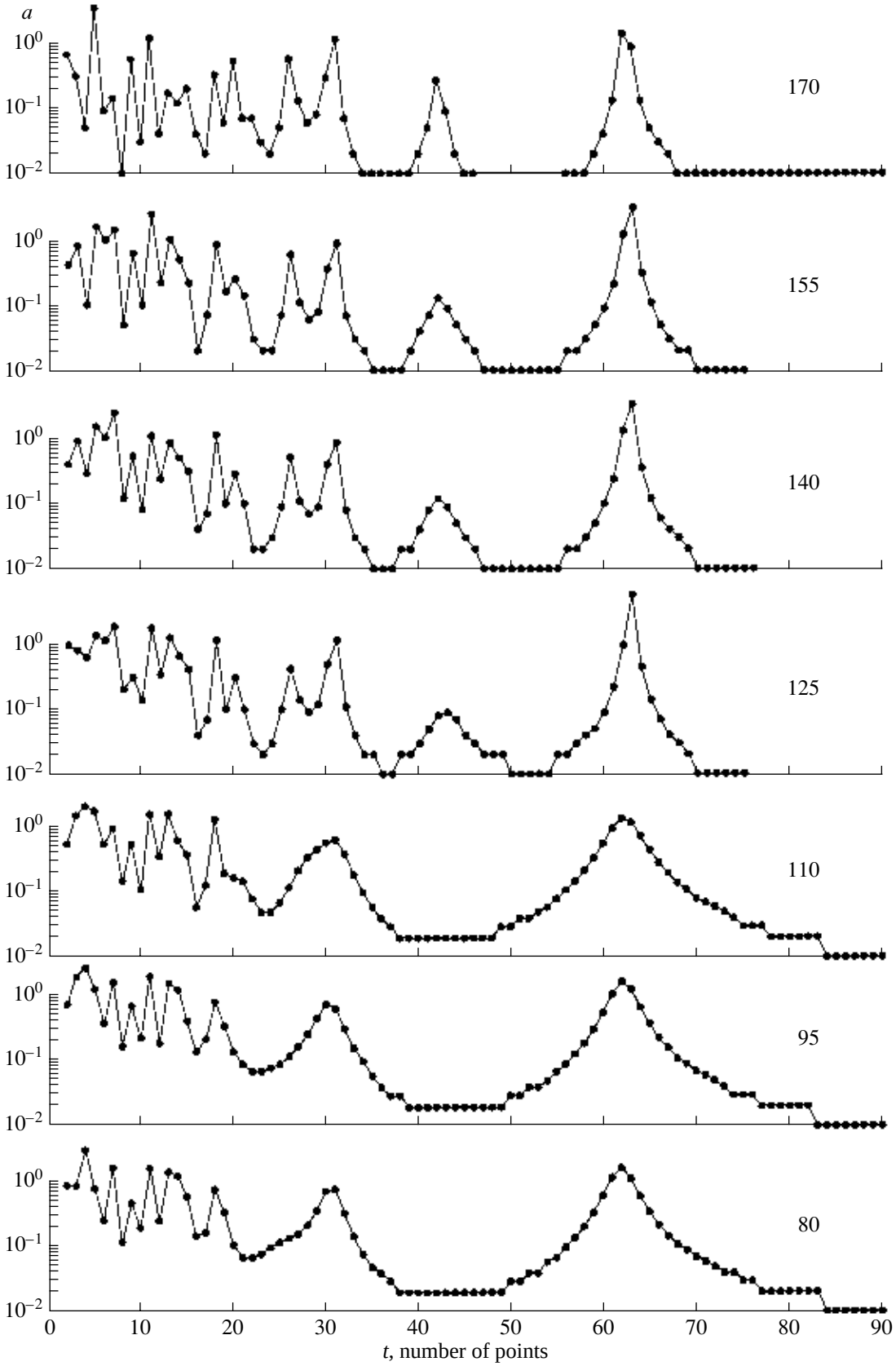

Fig. 3. Spectral diagrams of inclination in Matuyama rocks from profile 2 at various filter lengths *m*.

Table 1. Periods inferred from the MEM analysis applied to the time series of the geomagnetic time elements

Matuyama chron			Jaramillo subchron		
D	*I*	intensity	*D*	*I*	intensity
62100/3.6	56700/2.1	–	–	**53100/5.3**	–
–	–	**30200/0.22**	**40800/8.0**	–	–
31800/5.0	**25920/3.1**	–	–	29100/1.7	–
19980/6.6	19660/1.6	**21000/0.15**	**17250/6.5**	–	**20200/0.14**
–	**13180/3.1**	**13440/0.18**	–	14400/1.0	**13400/0.10**
9830/6.7	**11230/3.7**	–	–	10320/1.7	–
7020/4.9	–	**8820/0.12**	**7620/5.2**	–	**9200/0.08**
–	5600/2.3	**–/5100/0.18**	**5700/5.6**	**6080/3.6**	6200/0.07
4200/8.0	–	**4200/0.11**	**4000/4.2**	**4040/3.8**	4000/0.05
–	**3100/6.8**	–	–	**2620/3.7**	–
1725/3.5	**1850/1.7**	**2250/0.25**	**1840/6.5**	–	**2130/0.17**
–	**1470/4.0**	**1420/0.11**	**1410/4.9**	**1420/3.0**	**1520/0.18**
–	**1250/2.3**	–	1180/3.0	–	**1230/0.16**
1130/2.8	–	**1070/0.11**	–	**1050/3.1**	–
910/2.8	**885/2.3**	**930/0.16**	**820/5.5**	**860/3.0**	960/0.07
–	**830/3.1**	–	–	–	–
715/2.6	–	**740/0.09**	**700/4.3**	–	**700/0.10**
–	**640/3.4**	**680/0.11**	–	**660/1.8**	–
515/2.6	**540/2.5**	–	**570/4.2**	**550/2.3**	**520/0.14**
–	430/1.5	460/0.06	**450/3.4**	**450/2.6**	**440/0.11**
330/2.6	320/1.5	**320/0.13**	–	**340/2.3**	370/0.06
185/2.5	205/1.5	235/0.06	210/2.6	230/1.0	**200/0.08**

Note: The table entry is inferred period (in years)/oscillation amplitude. The declination (*D*) and inclination (*I*) amplitudes are given in arc degrees of the great circle, and the intensity amplitudes are given in relative units ($Rns \times 100$). Boldfaced are amplitudes whose significance level is greater than 90%.

length *m*. Figure 3 presents examples of the inclination spectra derived from the profile-2M data. Tables 1 and 2 summarize the MEM periods refined with the gradient descent method. The data from various parts of the section were grouped according to the similarity of their time characteristics. Boldfaced are the periods for which the significance level of the amplitude characteristic exceeds 90%. Of course, the grouping of the inferred periods is somewhat arbitrary.

B. *Results of the wavelet analysis*. The peaks recognized in the integral wavelet spectrum are summarized in Tables 2 and 3. To answer the question of which of these peaks correspond to real periodicities, we considered the wavelet decomposition $w(a, t)$. In terms of the wavelet analysis, this corresponds to horizontal structures (Figs. 4 and 5).

***D* spectrum.** The following peaks may be reliably considered to be quasi-periodic processes.

The Matuyama chron yielded a process with $a \approx$ 20700 years and a process beginning with $a \approx$ 1400 years and terminating with a period $a \approx 940$ years in the interval (–1150000 … –1140000) years (Figs. 4A1 and 5A1). Both these processes are reflected as peaks at 1080, 1600, and 20450 years in the integral spectrum. The integral spectrum also reveals a structure with $a \approx 9500$ years in the interval $t \in$ (–1140000 … –1090000) years and with $a \approx 4000$ years (Fig. 5A1; see also Table 3).

An accelerating process with $a \approx 21000 \longrightarrow$ 16000 years and a quasi-periodic, also accelerating, process with $a \approx 8400 \longrightarrow$ 3900 years and a maximum at $t \approx -1010000$ years are identified throughout the Jaramillo subchron interval. A process with $a \approx 39500$ is also likely to exist (Fig. 4B1). Likewise noticeable is a –1032000-year singularity corresponding to a vertical structure in spectrum in Fig. 5B1.

The remaining peaks in the time series under consideration are likely related to events that are local in time.

***I* spectrum.** Throughout the Matuyama chron interval, the wavelet diagrams (Fig. 4A2) reveal two (three) local events with $a \in$ (8400–15000) years, which may

Table 2. Periods (in years) inferred from the MEM and wavelet analyses applied to the time series of the magnetic scalar parameters of rocks

MEM analysis				Wavelet analysis			
Matuyama chron		Jaramillo subchron		Matuyama chron		Jaramillo subchron	
κ	IRM	κ	IRM	κ	IRM	κ	IRM
–	–	–	–	–	–	38800	37700
29500	–	–	–	–	30750	–	–
–	21500	21000	–	21450	21450	19400	–
16500	–	–	–	–	–	–	–
–	14150	13700	13650	13300	14300	14700	14300
–	9950	10650	–	–	–	–	–
8000	–	7950	–	–	–	–	8900
7100	6700	–	–	7300	–	7550	–
–	5500	–	5000	–	5450	–	–
4300	–	4330	3820	–	–	4330	4330
–	2670	3100	–	–	–	2900	3225
2200	–	–	–	–	–	–	–
1730	1800	1650	–	1850	1650	–	–
–	1430	1450	1350	–	–	–	–
1220	1290	1260	–	–	–	1275	–
1030	1030	1100	1115	–	1020	–	1095
900	815	815	–	945	–	–	–
725	–	–	750	–	–	–	–
–	640	670	–	–	–	–	650
590	–	550	590	–	580	–	–
470	–	460	500	–	–	480	–
–	330	385	380	300	320	–	360
–	190	230	150	–	180	–	150

be interpreted as a quasi-periodic process with an average period $a \in 11000$ years; structures with $a \in 22400$ years and a spectral maximum at $t \approx -1145000$ years. Moreover, a singularity with $a \approx 700$ years (Fig. 5A2), a quasi-periodic process with $a \approx 1400$ years over the interval $t \in (-1150000 \ldots -1145000)$ years, and a structure with $a \approx 2800$ years are identified.

Throughout the Jaramillo subchron interval, the wavelet decomposition of *I* (Fig. 4B2) is more irregular than the similar decomposition of *D* (Fig. 4B1). Only a poorly resolved process with $a \approx 26000$ years, a process with $a > 40000$ years that has no signature in the wavelet spectrum, and a few local maxima in the wavelet plane can be noted.

A weak periodicity with $a \approx 1125$ years with a superimposed process with $a \approx 1125 \longrightarrow 900$ years is present in an interval of the Jaramillo subchron (Fig. 5B2). This plot also reveals a process with $a \approx 3000$ years and a singularity at $t \approx 1034000$ years.

***Rns* spectrum.** The wavelet decomposition for the Matuyama chron reveals processes with $a \approx 18000 \longrightarrow 14000$ and $a \approx 22400$–28000 years (Fig. 4A3), local events with $a \approx 330$ years, weak periodicities with $a \approx 2200$ and 4400 years, and a structure with $a \approx 900$ years (Fig. 5A3). Two weak periodicities with $a \approx 19300$ and 29400 years (Fig. 4B3) and a horizontal structure with $a \approx 1125$–2250 years (Fig. 5B3) are superimposed on a local event ($a \approx 19300$ years, $t \approx -1050000$ years) in the Jaramillo subchron.

κ spectrum. The wavelet plane of the Matuyama chron exhibits a set of weakly expressed spots (Fig. 4A4), and only a process with $a \approx 1900$–2350 years is well resolved (Fig. 5A4).

In the case of the Jaramillo subchron, two local events with $a \approx 7600$ and 14300 years ($t \approx -1050000$ years), a

Table 3. Periods (in years) inferred from the wavelet analysis applied to the time series of the geomagnetic time elements

Matuyama chron			Jaramillo subchron		
D	*I*	intensity	*D*	*I*	intensity
39760	–	–	39780	–	–
–	–	–	–	–	30240
–	24080	26000	–	26300	–
20450	–	–	–	–	19300
–	–	–	17650	–	–
–	–	13600	–	15100	14300
9500	11200	9100	–	–	–
6700	7850	–	–	–	–
–	–	6000	5700	6200	6050
3900	–	4350	–	–	–
2750	3000	–	–	2900	–
–	–	2230	–	–	2000
1600	1410	–	1540	–	1500
1080	–	–	–	1125	–
–	–	900	–	900	–
–	660	–	750	–	–
540	–	–	–	–	–
–	–	–	–	–	450
320	–	320	345	360	–
190	180	–	–	180	170

Table 4. The most reliable periods (in years) derived from the analysis of wavelet diagrams

	Matuyama chron (chron zone)	Jaramillo subchron (subchron zone)
D	1400 ⟶ 940	–
	4000	–
	9500	8400 ⟶ 3900
	20700	21000 ⟶ 16000
	–	39500
I	1400	900–1125
	2800	3000
	11000	–
	22400	26000
	–	>40000
Rns	330	–
	900	–
	2200	1125–2250
	4400	–
	18000 ⟶ 14000	19300
	22400–28000	29400
k	1900–2350	2850
	–	19300
	–	38600
IRM	1900 ⟶ 1400	1125
	14000	13500
	–	38000

periodicity with $a \approx 19300$ years, superimposed on the latter, and a weak periodicity with $a \approx 38600$ years are noticeable (Fig. 4B4). Events with $a \approx 525$ and 1275 years at $t \approx -1034000$ years and a periodicity with $a \approx 2850$ years can also be noted (Fig. 5B4).

IRM spectrum. The Matuyama chron reveals a structure with $a \approx 14000$ years and a local event ($a \approx 3900$ years, $t \approx -1090000$).The large-scale spectrum is strongly irregular (Fig. 5A5), possibly indicating a process with $a \approx 1900 \longrightarrow 1400$ years. The Jaramillo subchron exhibits 1125-, 13450-, and 38000-year structures and a local event with $a \approx 4200$ years centered at $t \approx -1000000$ years (Figs. 4B5 and 5B5). Table 4 presents the most reliable periods derived from the wavelet analysis.

DISCUSSION OF RESULTS

1. Comparison of integral characteristics. The results of the above calculations based on two essentially different methods are presented in Tables 1 to 3. As evident from their comparison, the MEM analysis commonly reveals a greater number of periodicities, and most periodicities recognized from the wavelet analysis have analogues in the MEM results. The comparison between the MEM and wavelet periodicities provides morphological constraints on nearly energy one of the oscillations. However, the nonstationary behavior of the processes in question, which is evident from the analysis of the wavelet diagrams, not all of the inferred periodicities match real processes. In this respect, we do not think it appropriate to analyze field variations on the basis of data derived from the MEM analysis and integral wavelet spectra. We only note that, in high- and intermediate-frequency spectral intervals, both methods yield variations in geomagnetic field characteristics that are consistent with the archaeomagnetically constrained spectrum of variations [Burlatskaya, 1987].

To decide which of these periods match actual physical processes, evolution characteristics of the wavelet spectra should be examined.

2. Wavelet diagrams. The spectral behavior wavelet diagrams that are discussed below are shown in Figs. 4 and 5. Their common feature is the presence of many local events, or singularities (see also the time behavior of the values in question in Figs. 1 and 2). Since the duration of many events is comparable with or shorter

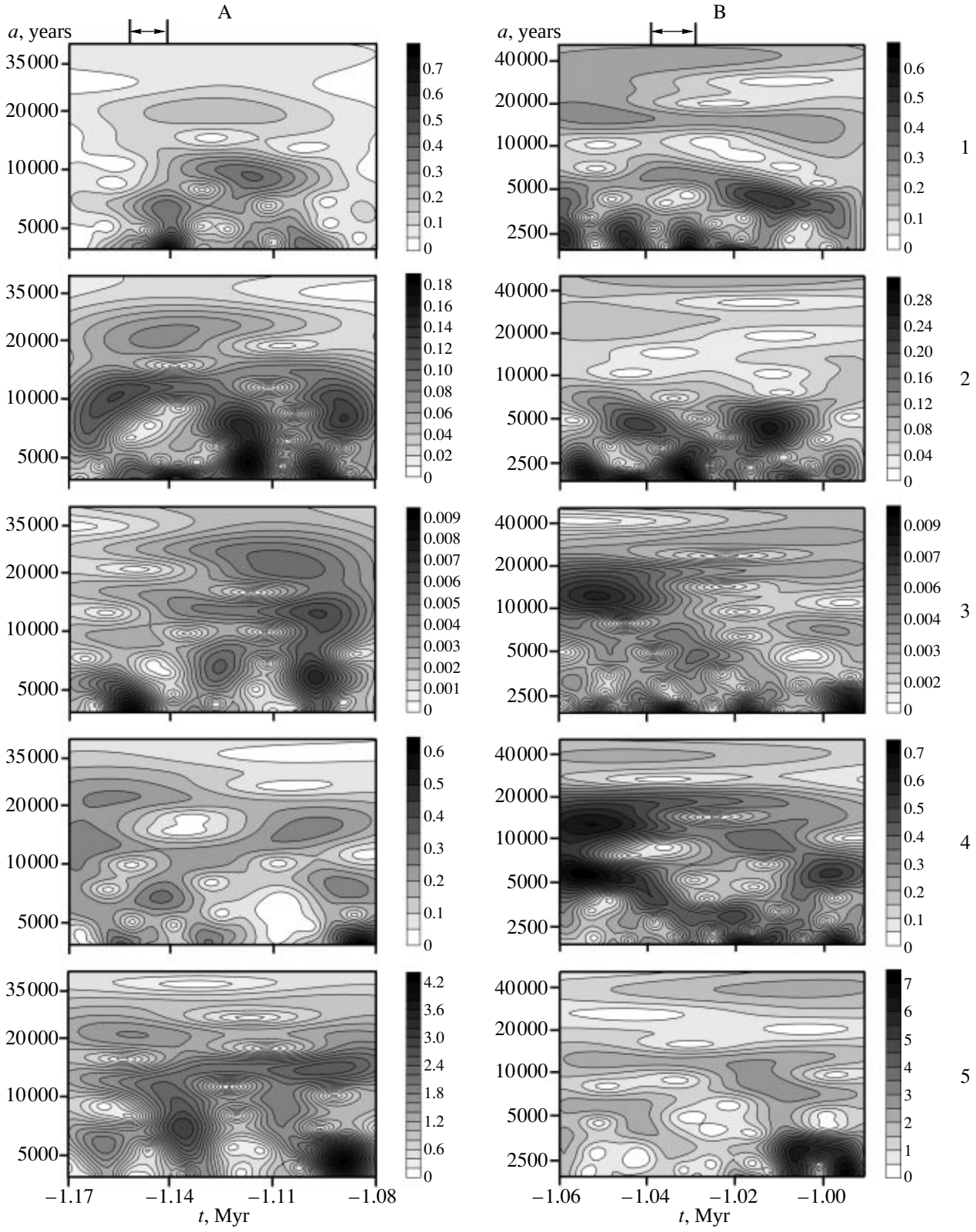

Fig. 4. Diagrams of spectral coefficients of the adaptive wavelets for the profile-1 data: A, Matuyama chron zone; B, Jaramillo subchron zone; 1, *D*; 2, *I*; 3, *Rns*; 4, κ; 5, IRM. *a* is the period on a logarithmic scale, and *t* is time on a linear scale. The right-hand columns are relative amplitude scales.

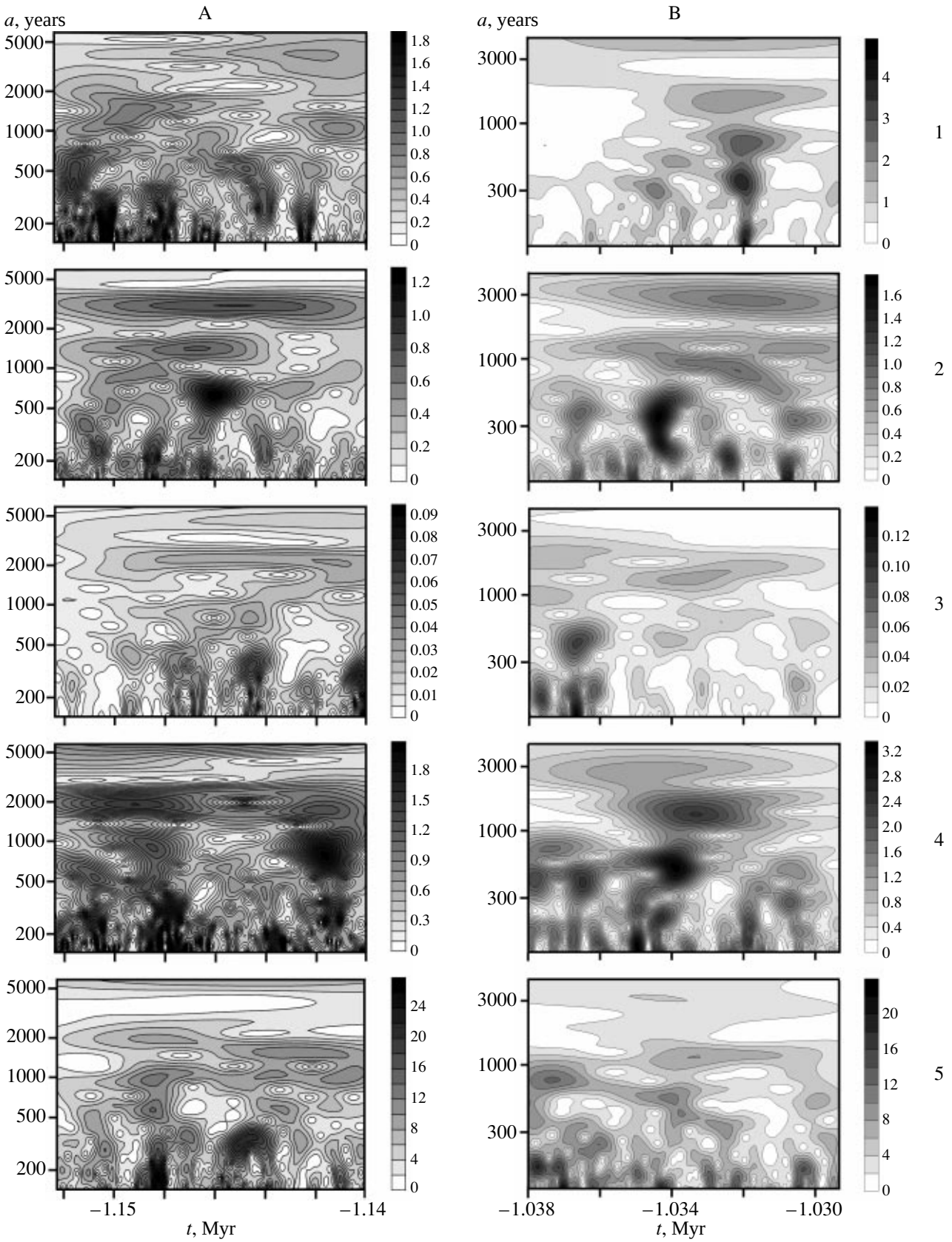

Fig. 5. Diagrams of spectral coefficients of the adaptive wavelets $w(a, t)$ for the profile-2 data. The notation is the same as in Fig. 4.

than the characteristic time of the processes, the latter cannot be regarded as actual periodicities. Table 4 presents the characteristic times that are shorter than the time intervals within which the related processes are observed. On average, only 1/5 of the periodicities presented in Tables 1 to 3 proved to be stable in time and may be attributed to real periodic processes. Based on the spectra identified in this way (Table 4), we compare the main features of the field behavior before and after the Matuyama–Jaramillo reversal.

The time spectra of the geomagnetic field components (*D*, *I*, *Rns*) and their amplitudes are not the same before and after the Matuyama–Jaramillo reversal. Nearly half of the periods recognized before the reversal are also observed after it, and *vice versa*. This difference may be caused by two factors. First, it may be due to data uncertainties related to an irregular sedimentation rate, missing data in the series, etc. Second, the time spectrum evolution itself is consistent with the theory of geomagnetic dynamo which explains the presence of characteristic times (200 kyr and more) that are longer than those obtained in this work [Hollerbach *et al.*, 1992; Anufriev *et al.*, 1994, 1997; Anufriev and Hejda, 1998]. In other words, the time intervals considered may be too short for the field characteristics to recover their steady-state values, and the differences in question are evidence of the actual field variation associated with the reversal. This problem can be solved more reliably after the analysis of the field characteristics in the immediate vicinity of and during the reversal, examination of longer time series, and substantiation of the inferred results by data gained from studies of other sections.

Differences in spectra before and after the reversal are also observed for some periods of scalar magnetic characteristics in rocks from the chron zones studied. Many researchers relate these changes to climatic processes [Jacobs, 1994]. Thus, 19.3- and 39-kyr periods of magnetic susceptibility are not observed in the Matuyama zone, and a 38-kyr period is lacking in the IRM from the Jaramillo zone. Some of the variations observed in these characteristics are possibly associated with similar variations in the magnetic field components, although the spectra of variations in the geomagnetic field as constrained by archaeomagnetic data and in the climate have much in common (particularly at intermediate frequencies).

Some periods of different field components do not coincide, which may be due to differences in the spatial morphology (symmetry properties) of the components and does not involve any difficulties in their interpretation [Petrova and Reshetnyak, 1999]. Some accelerating processes with decreasing $a(t)$ are observed. Note that a similar acceleration of processes in geomagnetic field variations was established in works by V.N. Vadkovskii (personal communication).

CONCLUSIONS

1. On the whole, the integral wavelet spectra obtained through the averaging of wavelet diagrams over time are generally consistent with the MEM spectra. However, the analysis of their time stability invalidates most (about 4/5) of the inferred periodicities that are likely to reflect singular (quasi-periodic) behavior of the series.

2. The inferred spectra are discrete.

3. On average, only half of the reliably established periods coincide for variations in different geomagnetic field components in each of the time intervals studied. This fully agrees with the modeling results obtained for the related characteristics.

4. A nearly similar pattern is derived from the comparison between the spectra of field elements before and after the Matuyama–Jaramillo reversal. In order to solve the stability problem of this variation, longer time series should be studied, and spectral data immediately pre- and postdating the reversal are required.

ACKNOWLEDGMENTS

We are grateful to S.V. Filippov, N.P. Rotanova, P.G. Frik, and D.K. Galyagin, who kindly provided us with their software packages for MEM and wavelet analyses. This work was supported by the International Science Foundation, grant nos. 56000 and 56300, and by the Russian Foundation for Basic Research, project nos. 94-05-17243, 97-05-64469, and 97-05-64797.

REFERENCES

Anufriev, A. and Sokoloff, D., Fractal Properties of Geodynamo Models, *Geophys. Astrophys. Fluid Dyn.*, 1994, vol. 74, pp. 207–215.

Anufriev, A.P., Reshetnyak, M.Yu., Sokolov, D.D., and Kheida, P., Evolution of the Geomagnetic Field in Terms of the αω-Dynamo Model, *Geomagn. Aeron.*, 1997, vol. 37, no. 2, pp. 91–95.

Berggren, W.A., Kent, D.V., Swisher III, C.C., and Aubry, M.A., A Revised Cenozoic Geochronology and Chronostratigraphy, *Geochronology Time Scales and Global Stratigraphic Correlation. SEPM Special Publication*, 1995, no. 54, pp. 129–212.

Burakov, K.S., Galyagin, D.K., Nachasova, I.E., *et al.*, Wavelet Analysis of Geomagnetic Field Variations over the Past 4000 Years, *Fiz. Zemli*, 1998, no. 9, pp. 83–88.

Burg, J.P., *A New Analysis for Time Series Data*, Enschede: Advances Study Institute in Signal Processing, 1968.

Burlatskaya, S.P., *Arkheomagnetizm. Izuchenie drevnego geomagnitnogo polya* (Archaeomagnetism: Study of the Ancient Geomagnetic field), Moscow: IFZ AN SSSR, 1987.

Filippov, S.V.,. M., Application of the Steepest Descent and Regularization Methods to the Determination of Signal Parameters and Trend, *Preprint of Inst. Terrestrial Magnetism, Ionosphere and Radiowave Propagation, USSR Acad. Sci.*, Moscow, 1985, no. 57(390), p. 9.

Galyagin, D.K. and Frik, P.G., Adaptive Wavelets: An Algorithm for Spectral Analysis of Signals Including Data Gaps, *Mat. Model. Sist. Protsessov*, 1996, no. 4, pp. 20–28.

Galyagin, D.K., Reshetnyak, M.Yu., Sokolov, D.D., and Frik, P.G., Scaling of the Geomagnetic Field and the Geomagnetic Polarity Time Scales, *Dokl. Ross. Akad. Nauk*, 1998, vol. 360, no. 4, pp. 541–544.

Gurarii, G.Z., Bagin, V.I., Garbuzenko, A.V., *et al.*, The Stationary Geomagnetic Field of the Matuyama Chron and Jaramillo Subchron from Western Turkmenistan, *Fiz. Zemli*, 2000, no. 1, pp. 33–49.

Holschneider, M., *Wavelets: An Analysis Tool*, Oxford: Oxford Univ. Press, 1995.

Hollerbach, R., Barenghi, C.F., and Jones, C.A., Taylor's Constraint in a Spherical αω-Dynamo, *Geophys. Astrophys. Fluid Dyn.*, 1992, vol. 67, pp. 3–11.

Jacobs, J.A., *Reversals of the Earth's Magnetic Field*, 2nd ed., Cambr. Univ. Press, 1994.

Nikolaev, N.P. and Gamburtsev, A.G., Eds., *Atlas vremennykh variatsii prirodnykh protsessov* (Atlas of Time Variations in Natural Processes), Moscow: Nauka, 1994.

Petrova, G.N. and Reshetnyak, M.Yu., On the Time Spectrum of the Secular Variation Field and Its Sources, *Fiz. Zemli*, 1999, no. 6, pp. 53–60.

Torresani, B., *Analyse Continue par Ondelettes.*, CNRS Editions, 1995.